Received: 22 April 2021 | Revised: 10 August 2021 | Accepted: 16 August 2021

DOI: 10.1111/micc.12726

REVIEW ARTICLE

Microcirculation WILEY

Capturing membrane trafficking events during 3D angiogenic development in vitro

Caitlin R. Francis | Erich J. Kushner

Department of Biological Sciences, University of Denver, Denver, Colorado, USA

Correspondence
Erich J. Kushner, Department of Biological Sciences, University of Denver, Denver, CO 80210, USA.
Email: Erich.Kushner@du.edu

Funding information
Work was supported by funding from the National Heart Lung Blood Institute (Grant R15HL156106-01A1, 1R56HL148450-01, R00HL124311) (E.J.K).

Abstract

Objectives: Vesicular trafficking dictates protein localization, functional activity, and half-life, providing a critically important regulatory step in tissue development; however, there is little information detailing endothelial-specific trafficking signatures. This is due, in part, to limitations in visualizing trafficking events in endothelial tissues. Our aim in this investigation was to explore the use of a 3-dimensional (3D) in vitro sprouting model to image endothelial membrane trafficking events.

Methods: Endothelial cells were challenged to grow sprouts in a fibrin bead assay. Thereafter, spouts were transfected with fluorescent proteins and stained for various cell markers. Sprouts were then imaged for trafficking events using live and fixed-cell microscopy.

Results: Our results demonstrate that fibrin bead sprouts have a strong apicobasal polarity marked by apical localization of proteins moesin and podocalyxin. Comparison of trafficking mediators Rab27a and Rab35 between 3D sprouts and 2D culture showed that vesicular carriers can be imaged at high resolution, exhibiting proper membrane polarity solely in 3D sprouts. Lastly, we imaged exocytic events of von Willebrand Factor and demonstrated a distinct imaging advantage for monitoring secretion events in 3D sprouts as compared with 2D culture.

Conclusions: Our results establish that the fibrin bead sprouting assay is well-suited for imaging of trafficking events during angiogenic growth.

KEYWORDS
angiogenesis, apical membrane, blood vessel, development, endothelial, endothelium, exocytosis, imaging, lumen, Rab27a, sprouting, trafficking, vascular, vesicle, von Willebrand factor, Weibel-Palade body

1 | INTRODUCTION

The process of early blood vessel formation, or angiogenesis, is critical to establish the requisite vasculature for organismal growth.[1] During angiogenesis, early blood vessels establish the canonical morphologies that define adult vasculature, namely long interconnected conduits providing a portal for blood flow.[2] Endothelial cells (ECs) are the initial building blocks of blood vessel development, forming small sprouts and capillary-like networks that progressively invade growing embryonic tissue. Our more recent ability to image gross angiogenic processes in both development and disease has unlocked many outstanding questions in the field. This has also been aided

Abbreviations: 2D, 2-dimensional; 3D, 3-dimensional; ECs, Endothelial cells; Podxl, Podocalyxin; vWF, Von Willebrand Factor; WPB, Weibel-Palade Body.

by the expanding wealth of transgenic animals as well as a multitude of cellular and molecular biology techniques. In addition, many processes that are uniquely governed by endothelial tissues and fundamental to their function remain to be discovered. In particular, membrane trafficking-based regulation of endothelial function is an underserved area of exploration in the field of angiogenesis that is largely dependent on sub-cellular imaging techniques to interrogate function.

Trafficking broadly refers to the vesicle-based transport and movement of proteins through the cell. This process is parsed into endocytic (outside material in), exocytic (inside material out), and recycling (moving between both endocytic and exocytic) pathways.[3-5] Rab GTPase proteins are the most recognized multifunctional mediators of all trafficking events, acting as an intracellular barcoding system with over 70 known family members.[6,7] Rab proteins attach to the outside of vesicles where they define intracellular trafficking routes.[8,9] Activated Rabs then recruit or bind to tissue-specific effectors which can then promote localization, signaling, and degradation of their cargo. For example, in ECs Rab27a is required for Weibel-Palade Body (WPB) apical membrane fusion and von Willebrand Factor (vWF) exocytosis.[10] Indeed, the breadth of function trafficking encompasses is far and wide, and may collectively represent the most dominant, yet esoteric, regulatory program in a protein's life cycle.[7,11,12] Taken as a whole, how endothelial tissues harness trafficking-based regulation is a major outstanding question in the field of blood vessel development and homeostasis.

Much of the seminal work in the field of membrane trafficking has been carried out in epithelial tissue.[13] This is in large part due to their large rectangular shape and spatially segregated apical and basal domains allowing for relatively easy imaging of processes at either membrane. Additionally, epithelial cells readily establish apicobasal polarity in 2-dimensional (2D) culture, thus do not require much in the way of physical or chemical cues to elicit a defined polarity axis.[14] By contrast, ECs are exceedingly flat exhibiting a mesenchymal morphology.[15] In some instances, the distance between the apical and basal domains in ECs is diffraction limited (≤500 nm), hindering imaging of either membrane surface. In 2D culture endothelial cells are highly migratory, setting up a defined planar cell polarity axis. However, when independent of a sprouting structure, ECs do not show a commitment to an apical and basal membrane identity. Because trafficking biology primarily entails movement of vesicular cargo, transcript levels of trafficking mediators are typically held at a constant, excluding the use of simple expression analysis to interrogate function. In this realm, the ability to visualize differential trafficking events to various membranes is paramount to understanding function. Unfortunately, in vivo imaging of endothelial trafficking events present a significant challenge, due to the relative thinness of ECs coupled with the requirement for a less magnified microscope objective (eg, 20× vs 60× lens) to span the tissue depth needed to capture blood vessels. Therefore, we believe the use of a 3D sprouting model is an excellent compromise between providing the necessary cellular cues to reproduce angiogenic morphodynamics with ample sub-cellular imaging accessibility to image trafficking events.

In this investigation, our aim was to explore the use of a 3D in vitro sprouting model to image and evaluate membrane trafficking events in two scenarios. First, our goal was to capture sub-cellular dynamics of apical proteins, in particular, Rab GTPases and their cargo, related to lumen biogenesis. Second, was to evaluate luminal exocytic events at the apical membrane. Our reasoning for choosing these trafficking events was twofold: (1) these events are hard-to-impossible to distinguish in most in vivo models; and (2) are typically evaluated using 2D culture. Using a fibrin bead sprouting assay, we demonstrate the utility of this 3D in vitro system for capturing endothelial-specific trafficking events. Methodologically, we demonstrate that endothelial sprouts develop parallel and close to the imaging window allowing for use of commonly equipped high-resolution objectives. Additionally, we show that lumen biogenesis and exocytic trafficking events are easily imaged in multicellular sprouts to a much greater extent than 2D culture. Overall, this work highlights a highly reproducible in vitro assay that provides a tailored imaging platform for exploring blood vessel-specific trafficking networks.

2 | MATERIALS AND METHODS

2.1 | Cell culture

Pooled Human umbilical vein ECs (HUVECs) were purchased from PromoCell and cultured in EGM-2 media (PromoCell Growth Medium, ready-to-use) for 2–5 passages. For experiments, glass-bottomed imaging dishes were exposed to deep UV light for 6 min and coated with Poly-D-Lysine (ThermoFisher) for a minimum of 20 min. Small interfering RNA (Thermo Fisher) was introduced into primary HUVEC using the Neon® transfection system (Thermo Fisher). Scramble and Rab27a siRNAs were purchased from (Thermo Fisher) and resuspended to a 10 μM stock concentration and used at 0.5 μM (see data supplement). Normal human lung fibroblasts (NHLFs, Lonza) and HEK-A (Thermo Fisher) were maintained in Dulbeccos Modified Medium (DMEM) supplemented with 10% fetal bovine serum and penicillin/streptomycin antibiotics. Both NHLFs and HEKs were used up to 15 passages. All cells were maintained in a humidified incubator at 37°C and 5% CO_2.

2.2 | Sprouting angiogenesis assay

Fibrin bead assay was performed as originally reported by Nakatsu et al. 2007.[16] Briefly, HUVECs were coated onto micro-carrier beads (Amersham) and plated overnight. SiRNA treatment or viral transduction was performed the same day the beads were coated. The following day, the EC-covered microbeads were embedded in a fibrin

matrix. Once the clot was formed, media was overlaid along with 100 000 NHLFs. Media was changed daily along with monitoring of sprout development.

2.3 | Plasmid constructs

The following constructs were procured for this study: GFP-Rab27A (gift from William Gahl; Addgene plasmid #89237); Rab35 (gift from Peter McPherson; Addgene plasmid #47424); Neo DEST (705-1) (gift from Eric Campeau & Paul Kaufman; Addgene plasmid #17392); pMDLg/pRRE (gift from Didier Trono; Addgene plasmid # 12251); pVSVG (gift from Bob Weinberg; Addgene plasmid #8454); psPAX2 (gift from Didier Trono; Addgene plasmid #12260); pShuttle-CMV (gift from Bert Vogelstein; Addgene plasmid #16403); and AdEasier-1 cells (gift from Bert Vogelstein; Addgene, #16399).

2.4 | Lentivirus and adenovirus generation

Lentivirus was generated by using the LR Gateway Cloning method.[17] Genes of interest and fluorescent proteins were isolated and incorporated into a pME backbone via Gibson reaction.[18] Following confirmation of the plasmid by sequencing, the pME entry plasmid was mixed with the destination vector and LR Clonase. The destination vector used in this study was pLenti CMV Neo DEST (705-1). Once validated, the destination plasmids were transfected with the three required viral protein plasmids: pMDLg/pRRE, pVSVG, and psPAX2 into HEK 293 cells. The transfected HEKs had media after 4 h and the viral media was harvested at day 3.

Adenoviral constructs and viral particles were created using the Adeasy viral cloning protocol.[19] Briefly, transgenes were cloned into a pShuttle-CMV plasmid via Gibson Assembly. PShuttle-CMV plasmids were then digested overnight with MssI (Thermo Fisher) and linearized pShuttle-CMV plasmids were transformed into the final viral backbone using electrocompetent AdEasier-1 cells. Successful incorporation of pShuttle-CMV construct into AdEasier-1 cells was confirmed via digestion with PacI (Thermo Fisher). 5000 ng plasmid was then digested at 37°C overnight, then 85°C for 10 min and transfected in a 3:1 polyethylenimine (PEI, Sigma):DNA ratio into 70% confluent HEK 293A cells (Thermo Fisher) in a T-25 flask.

Over the course of 2–4 weeks, fluorescent cells became swollen and budded off the plate. Once approximately 70% of the cells had lifted off the plate, the remaining cells were scraped off and centrifuged at 500x*g* for 5 min in a 15 ml conical tube. The supernatant was aspirated, and cells were resuspended in 1 ml PBS. Cells were then lysed by 3 consecutive quick freeze-thaw cycles in liquid nitrogen, spun down for 5 min at 500x*g*, and supernatant was added to 70% confluent T-75 flasks. Propagation continued and collection repeated for infection of 10–15 cm dishes. After collection and 4 freeze-thaw cycles of virus collected from 10 to 15 cm dishes, 8 ml viral supernatant was collected and combined with 4.4 g CsCl (Sigma) in 10 ml PBS. Solution was overlaid with mineral oil and spun at 100,000x*g* at 10°C for 18 h. Viral fraction was collected with a syringe and stored in a 1:1 ratio with a storage buffer containing 10 mM Tris, pH 8.0, 100 mM NaCl, 0.1 percent BSA, and 50% glycerol. HUVEC were treated with virus for 16 h at a 1/10 000 final dilution in all cell culture experiments.

2.5 | Quantification of trafficking proteins

Quantification of pHlourin-podocalyxin was determined by projecting images (both 2D and 3D cells/sprouts) in 3D using the FIJI 3D viewer function and visually identifying accumulation(s) of pHlourin-podocalyxin relative to various plasma membranes. Quantification of WPB number was performed by counting vWF puncta on a per cell basis in both 2D culture and 3D sprouts. In both culture conditions, WPB localization was determined by first identifying WPB accumulations (≥4 WPBs) or where the highest population resided in each individual cell. Second, images were rendered as a 3D projection as mentioned above and the WPB puncta were scored based on its most proximal membrane (eg, basal or apical). Secretion of vWF was scored visually by identifying whether vWF was in a lumen or contained within a cell. Actin stain determined cell and lumen boundaries.

2.6 | Immunofluorescence and microscopy

HUVECs in 2D culture were fixed with 4% paraformaldehyde for 7 min. ECs were then washed three times with PBS and permeabilized with 0.5% Triton-X (Sigma) for 10 min. After permeabilization, cells were washed three times with PBS. ECs were then blocked with 2% bovine serum albumin (BSA) for 30 min. Once blocked, primary antibodies were incubated for approximately 4–24 h. Thereafter, primary antibodies were removed, and the cells were washed 3 times with PBS. Secondary antibodies with 2% BSA were added and incubated for approximately 1–2 h, washed 3 times with PBS, and mounted on a slide for imaging.

For imaging the fibrin bead assay, fibroblasts were removed from the clot with a 1-min trypsin incubation. Following incubation, the trypsin was neutralized with DMEM containing 10% BSA, washed 3 times with PBS, and fixed using 4% paraformaldehyde for 40 min. After fixation, the clot was washed 4 times with PBS, permeabilized with 0.5% Triton-X for 2 h and then blocked with 2% BSA for 1 h prior to overnight incubation with primary antibodies. The following day, primary antibodies were removed, and the clot was washed 5 times with PBS and secondary antibody was added with 2% BSA and incubated overnight. Before imaging, the clot was washed 5 times with PBS. All primary and secondary antibodies are listed in the supplemental data. Images were taken on a Nikon Eclipse Ti inverted microscope equipped with a CSU-X1 Yokogawa spinning disc field scanning confocal system and a Hamamatsu EM-CCD digital camera. Images were captured using a Nikon Plan Apo 60× NA 1.40 oil

objective using Olympus type F immersion oil NA 1.518. All images were processed using ImageJ (FIJI).[20]

2.7 | Statistical analysis

Experiments were repeated a minimum of three times. Statistical analysis and graphing were performed using GraphPad Prism. Statistical significance was assessed with a Student's unpaired *t* test for a two-group comparison. Statistical significance set a priori at $p < .05$.

3 | RESULTS

3.1 | Generating 3-dimensional sprouts using the fibrin bead assay

To image endothelial-specific trafficking signatures, we employed a fibrin bead sprouting assay first described by Nakatsu et al.[21] In this assay, ECs are coated onto a micro-carrier bead and then embedded into a fibrin matrix. Following the addition of a fibroblast feeder layer, the ECs sprout into the surrounding matrix (Figure 1A).

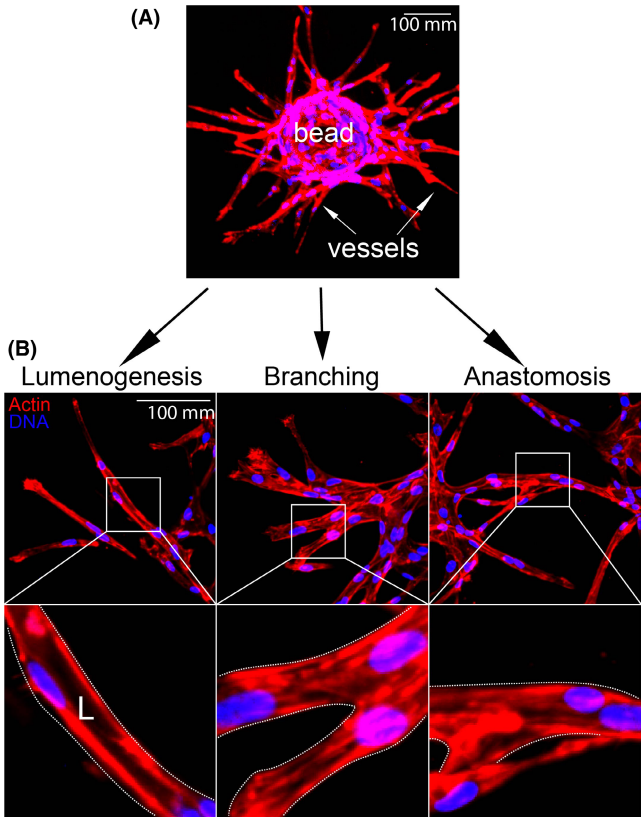

FIGURE 1 Fibrin bead assay recapitulates angiogenic traits in vitro. Top: representative image of embedded fibrin bead after 4 days of growth. Bottom: representative images of lumenogenesis, branching, and anastomosis with magnifications (boxes). L denotes lumen

Importantly, these sprouts produce multicellular proto-vessel structures, as opposed to solely filopodia invasion such as those observed in the Matrigel assay.[22] Here, sprouts reproduce characteristic in vivo sprouting features such as branching, dynamic cell shuffling,[23,24] anastomosis,[25] and lumen formation[21] (Figure 1B). There are other 3D sprouting assays that may demonstrate comparable sprouting characteristics; however, in our hands, the fibrin bead assay produced very distinct multicellular sprouts with a clearly defined tip and stalk cell morphology. This is important, as other assays can invade the surrounding matrix fashioning a cavernous lumen-like cavity, but this type of morphology can be primarily attributed to cyst formation, where the cells breakdown the matrix, but lack canonical sprouting characteristics.[26]

3.2 | 3D sprouts demonstrate a defined apical and basal polarity

To determine the suitability of the fibrin bead assay for trafficking studies, we first examined if sprout structures demonstrated apicobasal polarity when compared with 2D culture using standard confocal imaging techniques. To test this, 3D sprouts generated in the fibrin bead assay and ECs plated on coverslips (2D culture) were stained for actin (cytoskeleton), moesin (apical), beta-1 integrin (basal), VE-cadherin (junctional), and podocalyxin (Podxl, apical). 2D cultured cells demonstrated a diffuse distribution of moesin and Podxl with no clear plasma membrane enrichment, indicative of a lack of apicobasal polarity (Figure 2A). Orthogonal projections did not provide useful information as the axial resolution was far too low to make out individual puncta; therefore, we did not rely on this method going forward. In 2D, beta-1 integrin was localized to focal adhesions on the basal surface of the cell (Figure 2A). One interesting note is that ECs cultured on non-compliant surfaces, such as hard plastic or glass, spread out to a greater extent than cells cultured on soft matrices.[27] This elevated cell spreading in 2D could also contribute to the decreased separation between apical and basal surfaces, complicating discrete imaging of these membrane domains.

An immediate advantage of the fibrin bead system was that sprouts are oriented in such a manner to the imaging plane that the apical and basal membranes are captured in the X-Y plane as opposed to 2D cells, where the apical and basal domains are in the X-Z axial orientation. For example, 2D imaging of actin, VE-cadherin, Podxl, moesin, and beta-1 integrin in the conventional X-Y bottom-up view, these proteins are captured in high resolution (Figure 2A, top panel). However, in the orthogonal view, the proteins do not show proper apical membrane localization with Podxl and moesin not localizing to the dorsal surface (Figure 2A, bottom panel). Using a conventional oil 1.4 NA 60× objective with a working distance of 0.21 mm, we encountered no issues imaging 3D sprouting structures near the coverslip. In contrast to 2D culture, fibrin bead generated sprouts exhibited clearly polarized apical and basal membrane surfaces. For example, sprouts stained for actin and VE-cadherin demonstrated typical protein localization with actin throughout the cell

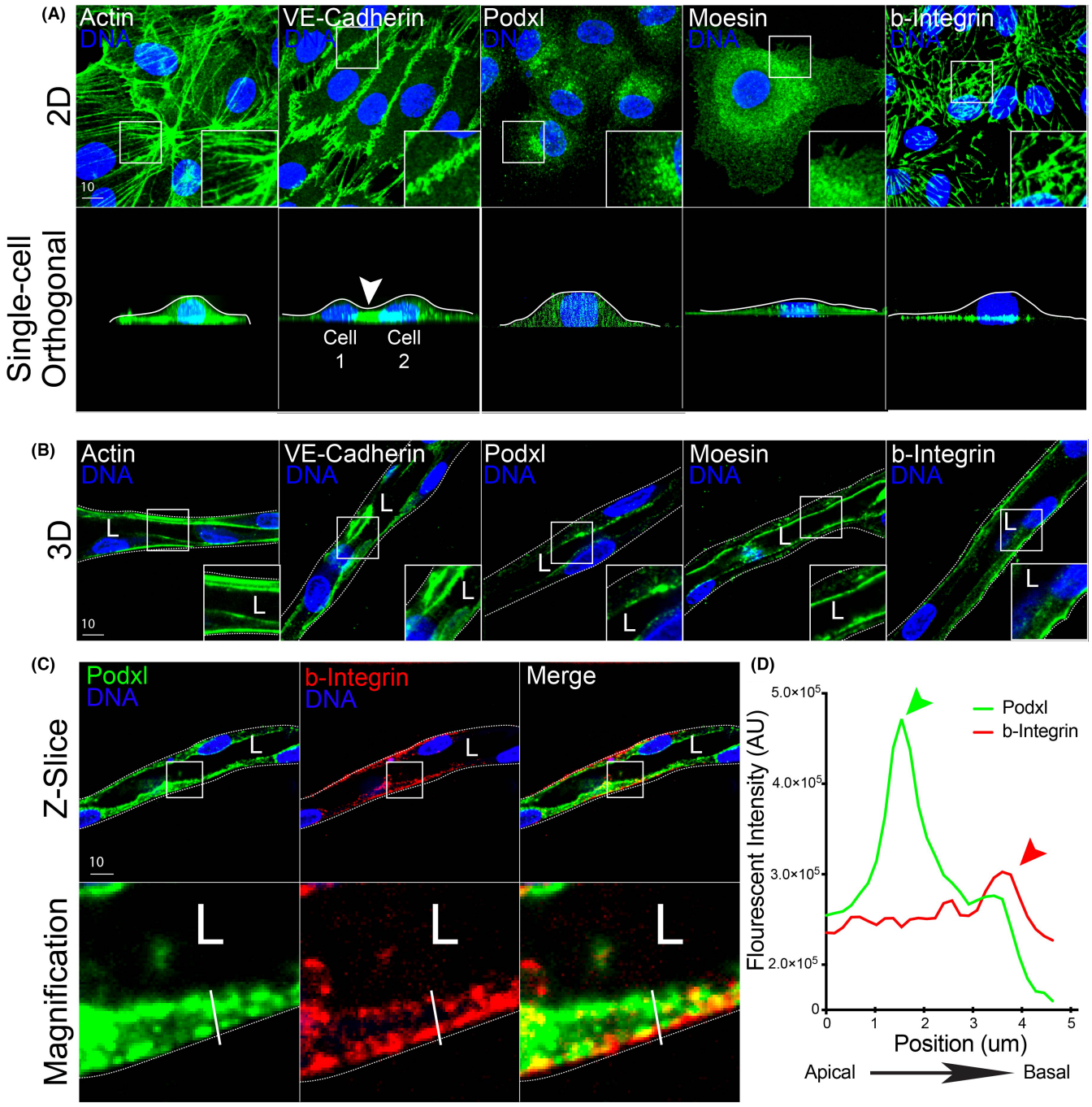

FIGURE 2 Comparison of cell polarity markers in 2D culture and 3D sprouts. (A) Representative images of endothelial cell cultured on 2D surface (top panels) and axial view (*x-z* plane, bottom panels). Cells were stained with actin (cytoskeleton), VE-cadherin (cell junctions), podocalyxin (Podxl, apical membrane), moesin (apical membrane), and beta-1 integrin (b-integrin, basal membrane). White lines mark apical surface and arrowhead denotes junction between two cells. (B) Representative images of fibrin bead generated sprouts stained for indicated proteins. (C) Representative imaging showing co-staining of Podxl and b-integrin within the same sprout cross-section to highlight differences in apical and basal domains. (D) Line scan illustrating peaks in fluorescent intensity of podxl and b-Integrin relative to apical and basal domains. The green arrowhead denotes peak of podxl and red arrowhead denotes peak of b-Integrin. The white line in panel (C) denotes the line scan area. White boxes are areas of magnification and while dotted lines indicated sprout boundaries. L denotes lumen

and VE-cadherin at cell-cell interfaces (Figure 2B). However, Podxl and moesin that did not localize to the apical surface in 2D culture, demonstrated robust apical localization in 3D sprouts, distinct from beta-1 integrin on the basal membrane (Figure 2B). Upon closer inspection, Podxl was highly enriched at the apical membrane and spatially segregated from beta-1 integrin on the basal surface in 3D sprouts (Figure 2C,D). In addition, we observed that ECs in sprouting structures displayed increased apical-basal membrane separation as

compared with cells cultured in 2D, this also enhanced our ability to distinguish these domains (Figure 2C,D). Overall, these results show fibrin bead generated sprouts demonstrate apical and basal signaling that can be imaged at high resolution.

3.3 | Dynamic Imaging of podocalyxin trafficking between 2D culture and 3D sprouting

Podxl is a glycoprotein that has been shown to be involved in lumen formation across many developmental models.[14] During lumen formation, Podxl is trafficked from the basal membrane to the apical membrane where it orchestrates delamination of the opposing cell membranes, creating the early lumen cavity.[28-31] Although many epithelial studies have documented Podxl's transcytosis, no endothelial studies have live-imaged this trafficking event to our knowledge. To image Podxl's insertion into the apical membrane, we constructed a pHluorin-tagged Podxl adenovirus (Figure 3A). PHluorin is a green fluorescent protein (GFP) variant that is non-fluorescent in acidified vesicles, but fluorescence is rescued at neutral pH following plasma membrane fusion (Figure 3A).[32] This approach allows us to differentiate between Podxl that is inserted into the plasma membrane from populations that reside in sub-apical vesicles. We first live-imaged pHluroin-Podxl (pH-Podxl) in 2D cultured ECs. Here, pH-Podxl was localized to discrete puncta and did not show any distinguishable membrane preference (Figure 3B,C; Movie S1); again, suggesting a lack of polarity. In 2D, we observed endocytosis of pH-Podxl marked by the sudden loss of pH-Podxl puncta on the membrane surface (Figure 3C). By contrast, live imaging of pH-Podxl in fibrin bead assay sprouts demonstrated a robust and uniform distribution of pH-Podxl that decorated the expanding lumen cavity. At sites of active membrane deadhesion at either end of the expanding lumen, we observed the greatest pH-Podxl intensity (Figure 3B,D; Movie S2). In line with previous reports,[33-36] our results demonstrate that Podxl is actively trafficked to the apical membrane; although, it may be trafficked more robustly to cell-cell interfaces actively undergoing membrane deadhesion via undescribed mechanisms. Overall, these data indicate that sub-cellular Podxl trafficking events can be captured at high resolution during vascular lumen formation.

3.4 | Characterizing Rab35 trafficking between 2D culture and 3D sprouting

Rab GTPases represent a class of well-studied proteins that orchestrate vesicle trafficking.[6,33,37] In particular, Rab35 has been shown to play a multitude of roles depending on the organism, tissue type and cellular conditions.[38-41] Also, Rab35's localization has not been characterized in vascular tissue. Thus, to explore the use of the fibrin bead assay for imaging endothelial trafficking events, we overexpressed Rab35 in both 2D and 3D culture conditions. In 2D culture, GFP-Rab35 displayed a membranous localization but was broadly distributed, not co-localizing with basal marker beta-1 integrin, and only partially with the cytoskeletal protein actin (Figure 4A). By contrast, expression of GFP-Rab35 in 3D fibrin bead sprouts demonstrated a preference for the apical membrane co-localizing with actin and distinct from beta-1 integrin (Figure 4C). In comparing line scans between 2D culture and the 3D sprouting model, we observed a defined accumulation of Rab35 at the apical membrane, while 2D culture did not demonstrate any membrane localization preference. These data suggest that the sprouting environment may be instructing Rab35 localization to the apical membrane.

Live imaging in 2D culture showed GFP-Rab35 localized to membrane protrusions and lamellipodia, but also showed a broad cytoplasmic and plasma membrane distribution. There was no membrane bias of Rab35 in 2D culture that was readily apparent (Figure 5A; Movie S3). Conversely, live imaging of Rab35 in the 3D sprouts revealed that, again, Rab35 is membranous but with a clear preference for the apical membrane (Figure 5B). Additionally, unique to the 3D sprouting environment, we could observe individual endosome movements adjacent to the apical membrane, which we could not detect in 2D culture (Figure 5B; Movie S4). Rab35 has previously been shown to take part in Rac1 signaling and endosome transport in other tissues,[42] our observed endosomal structures are consistent with those findings, but have never been reported in endothelial sprouts. Compared with 2D culture, the membrane dynamics were vastly dampened in 3D sprouting, suggesting culture in 2D may increase membrane dynamics consistent with other reports.[43] Overall, these data not only demonstrate a clear difference between Rab35 trafficking in 2D and 3D culture systems but shows the importance of fully resolving apical and basal domains to interrogate function.

3.5 | Capturing exocytic events between 2D culture and 3D sprouting

An endothelial-specific trafficking function is the secretion of clotting proteins, vWF into the luminal space upon injury.[44-46] WPBs are cigar-shaped vesicles that are rapidly deployed to the apical membrane to exocytose many components including pro-thrombotic vWF.[46] We sought to determine if tracking WPB-related secretion events in 3D sprouts were feasible. We believe this is important as the majority of reports examining WPB biology use 2D culture opposed to tracking exocytic events in 3D sprouts with a more physiologically defined apicobasal polarity. To do so, in 2D culture, we expressed GFP-Rab27a which has been previously shown to decorate WPBs.[34,47,48] Consistent with other reports, Rab27a strongly co-localized with vWF on WPB puncta.[34,47,48] Co-labeled WPB puncta were randomly distributed throughout the cell with no distinguishable membrane preference (Figure 6A). In 3D fibrin bead sprouts, Rab27a and vWF co-stained WPBs were easily visualized in proximity to apical or basal domains. In accordance with WPB function, we observed that WPBs accumulated at the apical membrane in many instances (Figure 6B). Interestingly, we observed that WPB number is generally increased in ECs within sprout structures as compared with ECs in 2D culture (Figure 6C). Of the WPBs in

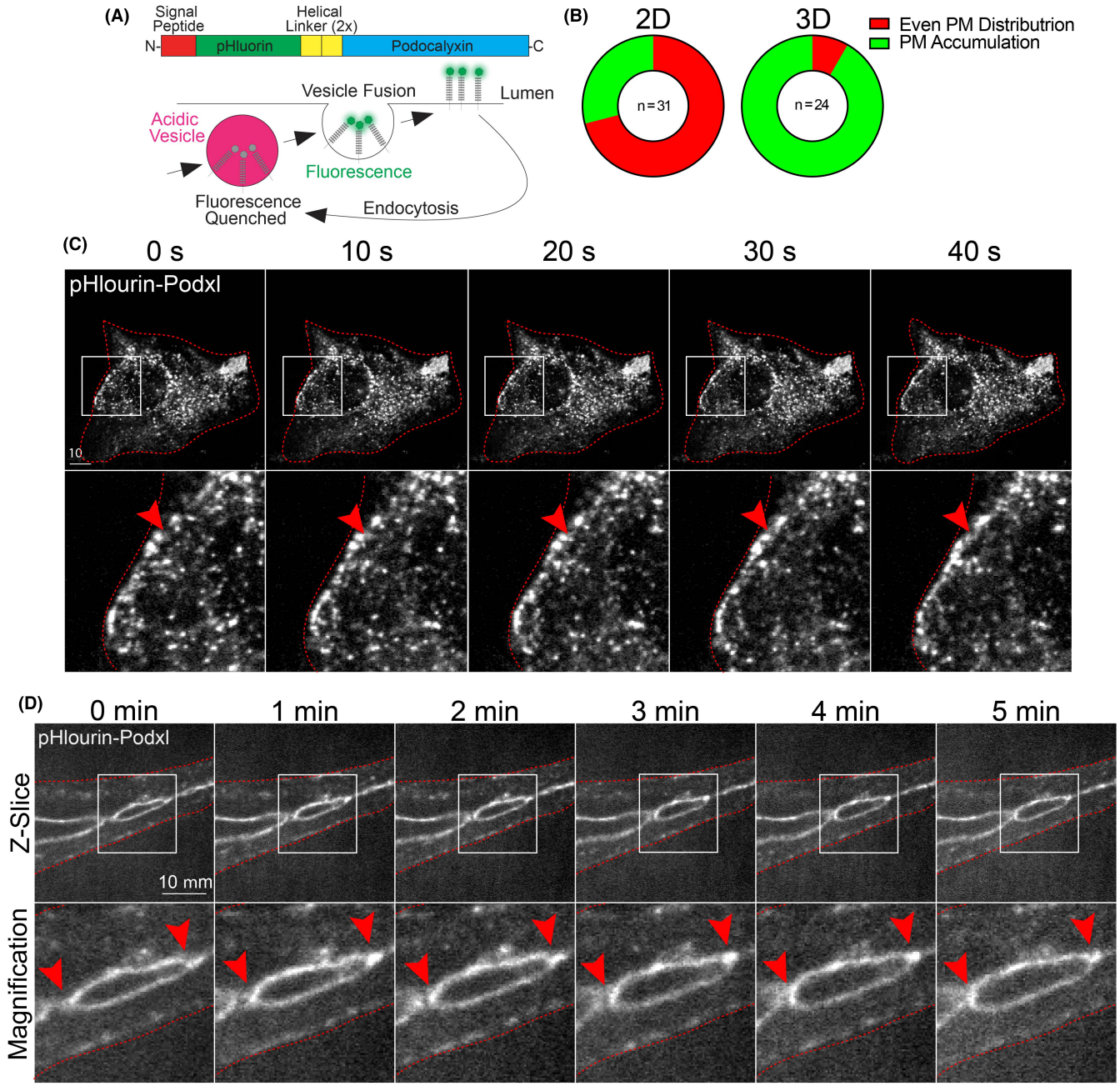

FIGURE 3 Live imaging of podocalyxin trafficking in 2D culture and 3D sprouts. (A) Structure of engineered pHluorin-Podxl fusion protein. In acidified vesicles, pHluorin fluorescence is significantly quenched. However, once inserted on the plasma membrane at neutral pH, fluorescence is rescued allowing for visualization of plasma membrane insertion. (B) Graph showing percentages of pHluorin-Podxl with either even or punctate plasma membrane (PM) distribution. (C) Live imaging of 2D cell expressing pHluorin-Podxl over time. Red arrowheads denote puncta accumulated at the leading edge of the cell. (D) Live imaging of fibrin bead generated sprout expressing pHluorin-Podxl over time. Red arrowheads indicate active areas of lumen expansion where Podxl is accumulating. White boxes are areas of magnification and red lines indicated sprout boundaries. L denotes lumen

2D plated cells, there was almost equal split between the number of WPB accumulations that were in close proximity to the basal domain (≤1 μm) and generally contained within the body of cytoplasm, with 10% of WPBs at the apical domain (Figure 6D). By contrast, ECs in a 3D sprout showed that 36% of WPB accumulations were near the apical domain, 50% in the cytoplasm, 0% at the basal domain with the remaining 17% exocytosed into the lumen cavity (Figure 6D). These results demonstrate that WPBs can be resolved in 3D sprouts.

Moving to live imaging of WPBs labeled with Rab27a in 2D, we easily resolve discrete puncta and the disappearance of individual WPBs, presumably being exocytosed (Figure 7A; Movie S5). In live-imaged 3D sprouts prior to lumen formation, we observed a substantial accumulation of WPBs at the cell-cell interface as previously

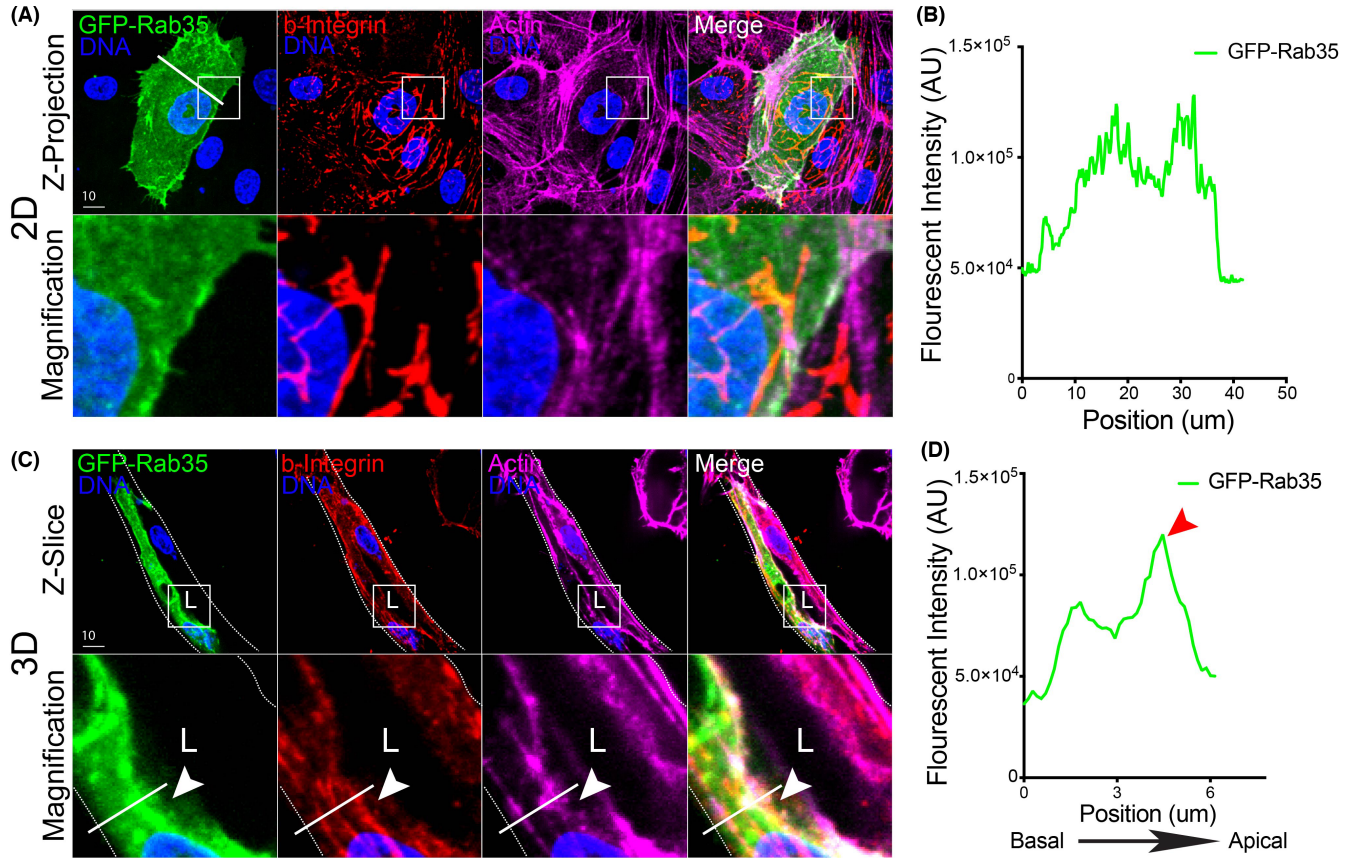

FIGURE 4 Visualizing Rab35 GTPase localization in 2D culture and 3D sprouts. (A) Representative image of endothelial cell expressing GFP-Rab35, stained for beta-1 integrin (b-integrin) and actin in 2D. Lower panels are magnification. While line is line scan area. (B) Line scan of Rab35 intensity in panel (A). White line across cell in panel (A) represents line scan location. (C) Representative image of fibrin bead sprout expressing GFP-Rab35, stained for b-integrin and actin. Arrowhead indicates Rab35 accumulation at apical membrane. While line is line scan area. (D) Line scan of Rab35 intensity in panel (C). Red arrowhead indicates border of apical membrane. White boxes are areas of magnification and while dotted lines indicated sprout boundaries. L denotes lumen

described by our group (Figure 7B; Movie S6).[34] Unlike 2D culture, we resolved WPBs aggregated at the apical membrane with less WPBs near the basal surface. We were then able to temporospatially track these structures relative to membrane domains (Figure 7B). These results demonstrate that in the fibrin bead sprouts, sub-cellular WPB puncta can be tracked with enough resolution that monitoring movements between apical and basal surfaces can be achieved. This is an important aspect of WPB biology, exocytosis will occur at the apical membrane.

Next, we compared exocytosis of WPB-housed vWF between 2D culture and fibrin bead sprouts. The rationale for this was as follows: (1) the primary function of vWF is to be secreted, thus we wanted to capture this process in a 3D multicellular sprout structure; and (2) for a direct comparison to the standard 2D exocytosis assay of vWF many others have employed.[10,48,49] In 2D culture, we knocked down Rab27a which has been shown to induce tonic vWF secretion.[10] In the Rab27a knockdown cells, there were qualitatively less vWF puncta as compared with the scrambled controls, although the amount of vWF exocytosis could not be assessed by imaging alone as it was secreted directly into the surrounding media (Figure 8A,C). By contrast, Rab27a knockdown in fibrin bead sprouts showed a dramatic accumulation of vWF effectively trapped within the sprout lumen (Figure 8B). We could reproduce this result by administration of ionomycin (Figure 8D,E), thus providing a conditional aspect to WPB evoked secretion. We believe this offers advantages over 2D culture in providing a better capacity to capture secretion events directed at the apical membrane in a growing sprout while simultaneously visualizing the relative amount of secreted protein(s) in the luminal space. These results show the utility of using a 3D sprouting culture system for visualizing secretion events.

4 | DISCUSSION

In the current investigation, we show that the fibrin bead sprouting assay has tremendous potential for imaging sub-cellular trafficking events. A primary disadvantage of in vivo imaging is the inability to capture trafficking processes due to the relative incompatibility of penetrating tissue with a long-working distance objective while maintaining high enough resolution to resolve sub-cellular processes. Additionally, in many in vivo models, capturing dynamic events at the spatial scales required to distinguish trafficking

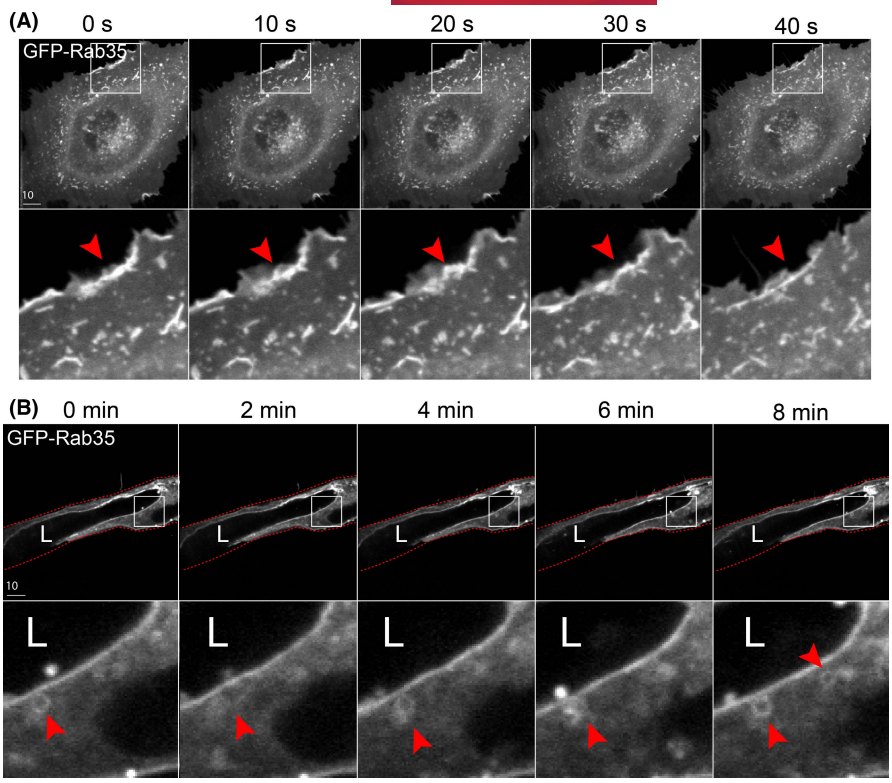

FIGURE 5 Live imaging of Rab35 trafficking in 2D culture and 3D sprouts. (A) Live imaging of cell expressing GFP-Rab35 over time. Red arrowheads denote puncta accumulated at the leading edge of the cell. (B) Live imaging of fibrin bead generated sprout expressing GFP-Rab35 over time. Red arrowheads indicate small endosome movements. White boxes are areas of magnification and red lines indicated sprout boundaries. L denotes lumen

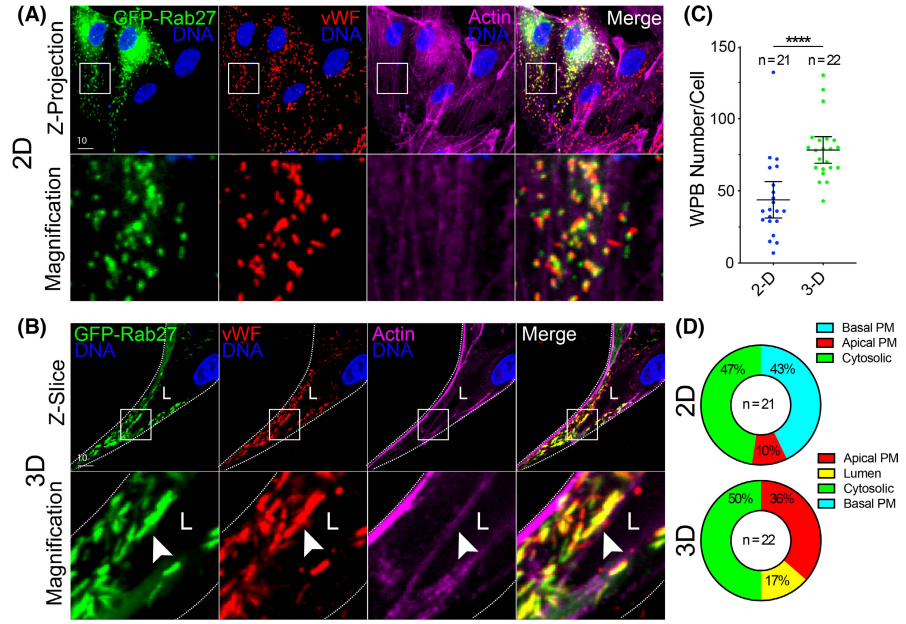

FIGURE 6 Imaging vWF exocytosis in 2D culture and 3D sprouts. (A) Representative images of endothelial cells in 2D culture expressing GFP-Rab27a and stained for von Willebrand Factor (vWF) and actin. (B) Representative images of a sprout expressing GFP-Rab27a and stained for vWF and actin. White arrowhead denotes Weibel-Palade Body accumulation. (C) Quantification of the number of vWF puncta between 2D culture and 3D sprouts. (D) Percentage of vWF accumulations (≥4 vWF puncta) that localize to a particular cellular location. PM = plasma membrane. *N* = number of cells. White boxes are areas of magnification and white dotted lines indicated sprout boundaries. L denotes lumen. Values are means ± SEM; significance: ****$p < .0001$. Statistical significance was assessed with an unpaired Students *t* test

processes is not feasible. A common workaround to these issues is 2D culture of ECs. However, our work establishes that this type of culture system strips away apicobasal signaling that is paramount to many trafficking processes. Our results using the fibrin bead model highlights a middle ground, where 3D sprouts that embody the most salient physiological characteristics of in vivo sprouting can be imaged at high resolution on common confocal microscope platforms. Importantly, we demonstrate that imaging 3D sprouts not only

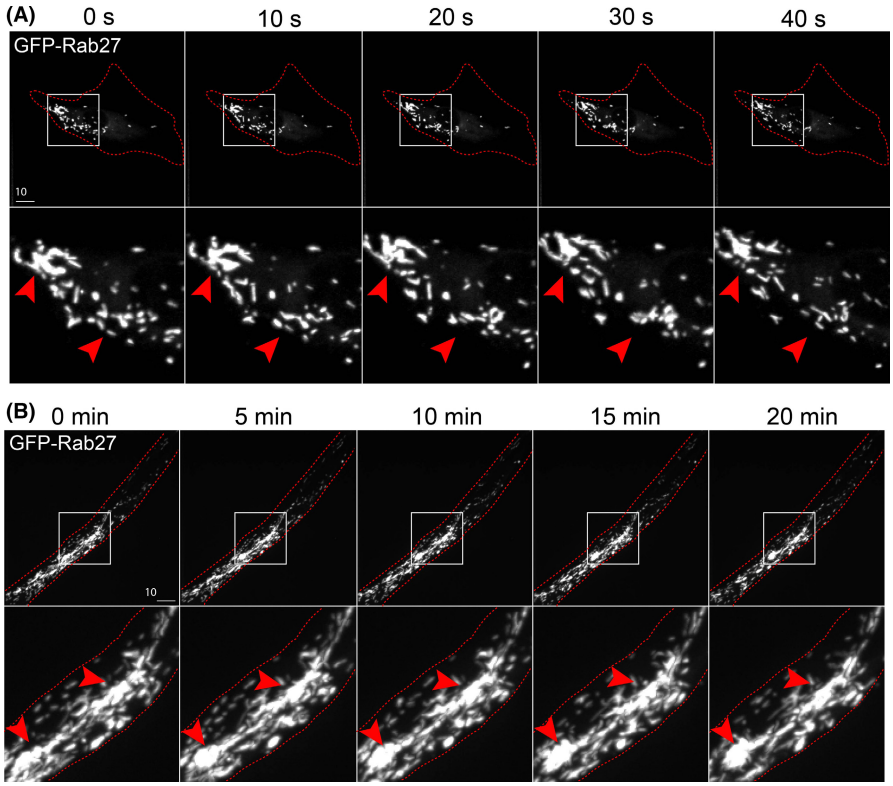

FIGURE 7 Live imaging of Weibel-Palade Body trafficking in 2D culture and 3D sprouting. (A) Live imaging of endothelial cells expressing GFP-Rab27a (Weibel-Palade Body marker) over time in 2D culture. Red arrowheads denote puncta accumulated at the leading edge of the cell. (B) Live imaging of fibrin bead generated sprout expressing GFP-Rab27a over time. Red arrowheads indicate accumulations of Weibel-Palade Bodies at cell-cell interface. White boxes are areas of magnification and red botted lines indicated cell boundaries. L denotes lumen

presents advantages in capturing apical and basal domains due to sprout orientation, but also is required to initiate proper apicobasal polarity. In the fibrin bead, we could clearly resolve trafficking mediators Rab35 and Rab27a both in live and fixed specimens and show their differential localization to the apical membrane. We also demonstrate the enhanced utility of the fibrin bead assay for imaging exocytic proteins that are sequestered in the luminal cavity. Overall, our results support that the fibrin bead sprouting model is suitable for visualizing endothelial trafficking events and could serve as an companion assay to in vivo work.

Our data comparing fibrin bead generated 3D sprouts with conventional 2D culture shows how trafficking events, such as those in lumen biogenesis or secretion, can be imaged in 3D sprout structures. By virtue of being able to capture a cross-section of the sprout long-axis, imaging apical and basal domains are very accessible as this is the natural X-Y plane (Figure 1). Conversely, the apicobasal orthogonal view in cells imaged on a 2D surface needs to be digitally reconstructed, limiting resolution. A problem that we originally envisioned was that the sprouts themselves would be too far from the coverslip, limiting the use of a high numerical aperture, low working distance objective. This was not the case, as most sprouts grew well within the working distance of a non–long-working distance 60× objective. Static imaging of cell polarity markers provided a strong indication that virtually no apical signaling is present in 2D culture when compared with 3D sprouts as luminal proteins moesin and podocalyxin did not localize to the apical domain (Figures 2 and 3). Depending on the experimental question, this may not be a major issue. For instance, imaging of cytoskeletal proteins, this would likely not pose a problem. However, an issue arises when testing processes that require apicobasal polarity that is otherwise non-existent in 2D culture. This lack of polarity was also obvious when imaging Rab35 as it demonstrated apical localization in 3D sprouts and random localization on membrane protrusions in 2D cells.

Surprisingly, we found that exocytosis of vWF was perfectly contained within the luminal cavity when using the fibrin bead assay (Figures 6 and 7). Imaging individual sprouts, we could very easily resolve discrete WPBs. Furthermore, the spatial dynamics of individual WPBs could be resolved, this is not different from 2D culture except that individual puncta could be tracked relative to a particular membrane domain. This allows for quantification of individual WPB secretion events as well as the relative exocytosis of proteins on a per sprout basis, given the secreted proteins are confined to the lumen cavity. In 2D culture, secreted proteins diffuse into the surrounding media blocking the ability to ascribe local secretion events to a particular group of cells. Given the preponderance of literature investigating WPB trafficking function using 2D culture, the fibrin bead assay may be very beneficial in providing a more physiological component to these studies.

Culturing ECs in 3D matrixes to induce sprouting behaviors is not new to the field of angiogenesis. Assays such as the Matrigel,[22] vasculogenic assay,[29,50,51] hanging-drop,[52,53] and fibrin bead methods were initially used to investigate differences in endothelial sprouting and branching characteristics. For these types of gross morphometric analyses, these assays are still widely used, although there are major advantages and disadvantages to each method. What has changed in more recent years is a focus on cell-autonomous molecular mechanisms of sprouting angiogenesis that require an ever-expanding need to visualize sub-cellular processes. In this regard, our group heavily employs the fibrin bead assay for imaging trafficking pathways and has been continuously impressed

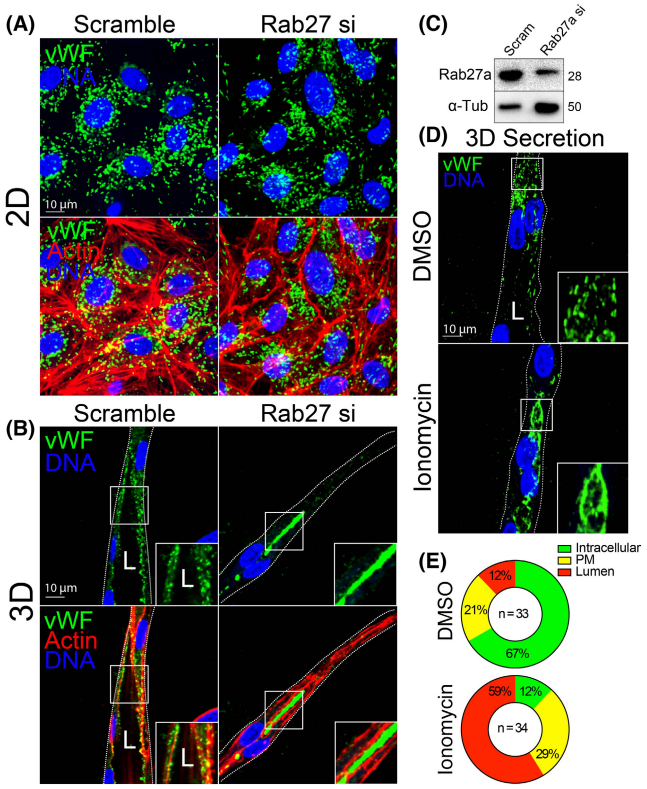

FIGURE 8 Monitoring exocytic events between 2D culture and 3D sprouting. (A) Representative 2D culture of endothelial cells stained for von Willebrand Factor (vWF) and actin treated with scramble or Rab27a-targeting siRNA (si). (B) Representative 3D fibrin bead generated sprout stained for vWF and actin treated with scramble or Rab27a-targeting siRNA. (C) Western blot confirmation of Rab27a knockdown efficiency. (D) Representative 3D fibrin bead generated sprout stained for vWF and treated with DMSO (vehicle) or ionomycin to induced Weibel-Palade Body exocytosis. (E) Percentage of intracellular or lumen trapped vWF between indicated conditions. *N* = number of cells. White boxes are areas of magnification and white dotted lines indicated sprout boundaries. L denotes lumen

by the functional disparities between 3D sprouting and 2D culture systems. The differences in signaling between 2D plated cells and 3D sprouts can be quite extreme in so far that no changes are detected in 2D culture (eg, no alterations in cell motility or polarity markers), but sprouting behaviors are greatly perturbed. Not detecting differences makes sense if the 2D culture system does not provide apicobasal signaling cues, then perturbations in this polarity axis will not be readily apparent and lost to the investigator. A possible drawback to this in vitro system is the lack of blood flow-based morphodynamic cell rearrangements. Several groups have published microfluidic devices that incorporate fluid flow that could be potentially substituted here.[54,55] Although, given the relative ease and low cost of the fibrin bead assay, it is likely more accessible to the average laboratory. Additionally, many developmental trafficking events, such as those in lumen biogenesis, precede blood flow, thus a "flow-less" model would be appropriate in these circumstances.

Our endorsement of the fibrin bead sprouting assay does not exclude the possibility of other in vitro angiogenic or vasculogenic assays for imaging trafficking events as well as some in vivo models. For example, Davis et al. have demonstrated the excellent utility of the vasculogenic EC assay for not only tracking sprouting parameters, but also visualizing sub-cellular processes like cytoskeletal proteins and caveolin localization.[50,56,57] Since the fibrin bead assay uses micro-carrier beads, a system like the vasculogenic assay that makes de novo cord structures, where cells are engulfed by extracellular matrix, may more accurately recapitulate some stages of early blood vessel formation. Likewise, the original group who created the fibrin bead assay has also engineered a microfluidic sprouting system that could be very interesting for investigating trafficking patterns with flow.[55] For in vivo models, unlike mammalians, zebrafish are optically transparent early in development allowing for live imaging of blood vessel processes.[58-61] Many sub-cellular structures in ECs can be distinguished using this model; however, in our hands, we cannot yield the resolution required to confidently quantify subtle trafficking localization events using needed 20× and 40× long-working distance objectives. Therefore, we believe having the fibrin bead assay to complement an in vivo model can help bridge deficits in either approach. There are many others who have developed comparable blood vessel sprouting-related assays that may be suited for imaging trafficking events that we have not mentioned. Our primary aim in the current investigation was to report our overwhelmingly positive experience with the fibrin bead assay for imaging trafficking-related programs during angiogenic sprouting.

In conclusion, our data demonstrate that the fibrin bead sprouting assay is an excellent platform for imaging endothelial trafficking events, particularly those related to apical and basal domains. We believe this method is a good substitute for 2D culture on many levels, most notably for imaging endothelial-related trafficking behaviors. In this vein, we show the fibrin bead is a powerful assay for investigating lumen biogenesis trafficking, but this method could also extend to vascular endothelial growth factor receptor endocytosis research.[62] Likewise, this system and the accompanying imaging modalities would likely be well-suited for investigating tip vs stalk cell trafficking as Delta/Notch signaling employs various trafficking pathways. Trafficking aside, this general approach could be adopted to simply better image protein or cellular temporospatial dynamics during sprouting angiogenesis. Overall, we believe that endothelial-specific trafficking signatures represent a novel level of regulation that significantly contributes to vascular form and function. Moreover, tools that aid in characterizing these processes will allow researchers to answer novel questions related to endothelial biology.

5 | PERSPECTIVES

- Intracellular trafficking may play a formative role in blood vessel morphogenesis; however, these programs remain elusive due to difficulties in imaging these intricate sub-cellular processes.

- The fibrin bead assay provides a useful platform to generate sprouts that reliably forms apical and basal membrane identities to a significantly greater extent than 2D culture, while also allowing for visualization of trafficking events.
- The ability to image trafficking events during sprouting angiogenesis will significantly expand our understanding of how EC harness trafficking signaling networks during blood vessel development.

ACKNOWLEDGMENTS

The authors would like to thank Makenzie Bell and Marina Skripnichuk for critical reading of the manuscript.

CONFLICT OF INTEREST

None.

AUTHOR CONTRIBUTIONS

C.R.F performed all experiments. C.R.F and E.J.K wrote the manuscript.

ORCID

Erich J. Kushner https://orcid.org/0000-0002-1355-9511

REFERENCES

1. Bussmann J, Wolfe SA, Siekmann AF. Arterial-venous network formation during brain vascularization involves hemodynamic regulation of chemokine signaling. *Development*. 2011;138(9):1717-1726.
2. Kushner EJ, Bautch VL. Building blood vessels in development and disease. *Curr Opin Hematol*. 2013;20(3):231-236.
3. Farquhar MG. Multiple pathways of exocytosis, endocytosis, and membrane recycling: validation of a Golgi route. *Fed Proc*. 1983;42(8):2407-2413.
4. Orzech E, Cohen S, Weiss A, Aroeti B. Interactions between the exocytic and endocytic pathways in polarized Madin-Darby canine kidney cells. *J Biol Chem*. 2000;275(20):15207-15219.
5. Foley K, Boguslavsky S, Klip A. Endocytosis, recycling, and regulated exocytosis of glucose transporter 4. *Biochemistry*. 2011;50(15):3048-3061.
6. Agola JO, Jim PA, Ward HH, BasuRay S, Wandinger-Ness A. Rab GTPases as regulators of endocytosis, targets of disease and therapeutic opportunities. *Clin Genet*. 2011;80(4):305-318.
7. Hutagalung AH, Novick PJ. Role of Rab GTPases in membrane traffic and cell physiology. *Physiol Rev*. 2011;91(1):119-149.
8. Segev N. GTPases in intracellular trafficking: an overview. *Semin Cell Dev Biol*. 2011;22(1):1-2.
9. Mizuno-Yamasaki E, Rivera-Molina F, Novick P. GTPase networks in membrane traffic. *Annu Rev Biochem*. 2012;81:637-659.
10. Bierings R, Hellen N, Kiskin N, et al. The interplay between the Rab27A effectors Slp4-a and MyRIP controls hormone-evoked Weibel-Palade body exocytosis. *Blood*. 2012;120(13):2757-2767.
11. Jovic M, Sharma M, Rahajeng J, Caplan S. The early endosome: a busy sorting station for proteins at the crossroads. *Histol Histopathol*. 2010;25(1):99-112.
12. Tian T, Zhu Y-L, Hu F-H, et al. Dynamics of exosome internalization and trafficking. *J Cell Physiol*. 2013;228(7):1487-1495.
13. Weisz OA, Rodriguez-Boulan E. Apical trafficking in epithelial cells: signals, clusters and motors. *J Cell Sci*. 2009;122(Pt 23):4253-4266.
14. Mrozowska PS, Fukuda M. Regulation of podocalyxin trafficking by Rab small GTPases in 2D and 3D epithelial cell cultures. *J Cell Biol*. 2016;213(3):355-369.
15. Dudley AC. Tumor endothelial cells. *Cold Spring Harb Perspect Med*. 2012;2(3):a006536.
16. Nakatsu MN, Davis J, Hughes CC. Optimized fibrin gel bead assay for the study of angiogenesis. *J Vis Exp*. 2007;3:186. https://doi.org/10.3791/186. Epub 2007 Apr 29.
17. Campeau E, Ruhl VE, Rodier F, et al. A versatile viral system for expression and depletion of proteins in mammalian cells. *PLoS One*. 2009;4(8):e6529.
18. Gibson DG, Young L, Chuang R-Y, Venter JC, Hutchison CA, Smith HO. Enzymatic assembly of DNA molecules up to several hundred kilobases. *Nat Methods*. 2009;6(5):343-345.
19. He TC, Zhou S, da Costa LT, Yu J, Kinzler KW, Vogelstein B. A simplified system for generating recombinant adenoviruses. *Proc Natl Acad Sci U S A*. 1998;95(5):2509-2514.
20. Schneider CA, Rasband WS, Eliceiri KW. NIH Image to ImageJ: 25 years of image analysis. *Nat Methods*. 2012;9(7):671-675.
21. Nakatsu MN, Sainson RCA, Aoto JN, et al. Angiogenic sprouting and capillary lumen formation modeled by human umbilical vein endothelial cells (HUVEC) in fibrin gels: the role of fibroblasts and Angiopoietin-1. *Microvasc Res*. 2003;66(2):102-112.
22. Crabtree B, Subramanian V. Behavior of endothelial cells on Matrigel and development of a method for a rapid and reproducible in vitro angiogenesis assay. *Vitro Cell Dev Biol Anim*. 2007;43(2):87-94.
23. Kushner EJ, Ferro LS, Yu Z, Bautch VL. Excess centrosomes perturb dynamic endothelial cell repolarization during blood vessel formation. *Mol Biol Cell*. 2016;27(12):1911-1920.
24. Jakobsson L, Franco CA, Bentley K, et al. Endothelial cells dynamically compete for the tip cell position during angiogenic sprouting. *Nat Cell Biol*. 2010;12(10):943-953.
25. Nesmith JE, Chappell JC, Cluceru JG, Bautch VL. Blood vessel anastomosis is spatially regulated by Flt1 during angiogenesis. *Development*. 2017;144(5):889-896.
26. Dubois-Stringfellow N, Jonczyk A, Bautch VL. Perturbations in the fibrinolytic pathway abolish cyst formation but not capillary-like organization of cultured murine endothelial cells. *Blood*. 1994;83(11):3206-3217.
27. Engler A, Bacakova L, Newman C, Hategan A, Griffin M, Discher D. Substrate compliance versus ligand density in cell on gel responses. *Biophys J*. 2004;86(1 Pt 1):617-628.
28. Bryant DM, Roignot J, Datta A, et al. A molecular switch for the orientation of epithelial cell polarization. *Dev Cell*. 2014;31(2):171-187.
29. Davis GE, Cleaver OB. Outside in: inversion of cell polarity controls epithelial lumen formation. *Dev Cell*. 2014;31(2):140-142.
30. Meder D, Shevchenko A, Simons K, Füllekrug J. Gp135/podocalyxin and NHERF-2 participate in the formation of a preapical domain during polarization of MDCK cells. *J Cell Biol*. 2005;168(2):303-313. Epub 2005 Jan 10.
31. Yasuda T, Saegusa C, Kamakura S, Sumimoto H, Fukuda M. Rab27 effector Slp2-a transports the apical signaling molecule podocalyxin to the apical surface of MDCK II cells and regulates claudin-2 expression. *Mol Biol Cell*. 2012;23(16):3229-3239.
32. Sankaranarayanan S, De Angelis D, Rothman JE, Ryan TA. The use of pHluorins for optical measurements of presynaptic activity. *Biophys J*. 2000;79(4):2199-2208.
33. Bryant DM, Datta A, Rodríguez-Fraticelli AE, Peränen J, Martín-Belmonte F, Mostov KE. A molecular network for de novo generation of the apical surface and lumen. *Nat Cell Biol*. 2010;12(11):1035-1045.
34. Francis CR, Claflin S, Kushner EJ. Synaptotagmin-like protein 2a regulates angiogenic lumen formation via Weibel-Palade body apical secretion of angiopoietin-2. *Arterioscler Thromb Vasc Biol*. 2021;17(4):435-437.
35. Strilić B, Eglinger J, Krieg M, et al. Electrostatic cell-surface repulsion initiates lumen formation in developing blood vessels. *Curr Biol*. 2010;20(22):2003-2009.

36. Strilic B, Kučera T, Eglinger J, et al. The molecular basis of vascular lumen formation in the developing mouse aorta. *Dev Cell*. 2009;17(4):505-515. https://doi.org/10.1016/j.devcel.2009.08.011
37. Grosshans BL, Ortiz D, Novick P. Rabs and their effectors: achieving specificity in membrane traffic. *Proc Natl Acad Sci U S A*. 2006;103(32):11821-11827.
38. Allaire PD, Marat AL, Dall'Armi C, Di Paolo G, McPherson PS, Ritter B. The Connecdenn DENN domain: a GEF for Rab35 mediating cargo-specific exit from early endosomes. *Mol Cell*. 2010;37(3):370-382.
39. Klinkert K, Echard A. Rab35 GTPase: a central regulator of phosphoinositides and F-actin in endocytic recycling and beyond. *Traffic*. 2016;17(10):1063-1077.
40. Shaughnessy R, Echard A. Rab35 GTPase and cancer: linking membrane trafficking to tumorigenesis. *Traffic*. 2018;19(4):247-252.
41. Villagomez FR, Medina-Contreras O, Cerna-Cortes JF, Patino-Lopez G. The role of the oncogenic Rab35 in cancer invasion, metastasis, and immune evasion, especially in leukemia. *Small GTPases*. 2018;11(5):334-345.
42. Zhu Y, Shen T, Liu J, et al. Rab35 is required for Wnt5a/Dvl2-induced Rac1 activation and cell migration in MCF-7 breast cancer cells. *Cell Signal*. 2013;25(5):1075-1085.
43. Gardel ML, Schneider IC, Aratyn-Schaus Y, Waterman CM. Mechanical integration of actin and adhesion dynamics in cell migration. *Annu Rev Cell Dev Biol*. 2010;26:315-333.
44. Hattori R, Hamilton KK, Fugate RD, McEver RP, Sims PJ. Stimulated secretion of endothelial von Willebrand factor is accompanied by rapid redistribution to the cell surface of the intracellular granule membrane protein GMP-140. *J Biol Chem*. 1989;264(14):7768-7771.
45. Lillicrap D. von. Willebrand disease: advances in pathogenetic understanding, diagnosis, and therapy. *Blood*. 2013;122(23):3735-3740.
46. Nightingale TD, McCormack JJ, Grimes W, et al. Tuning the endothelial response: differential release of exocytic cargos from Weibel-Palade bodies. *J Thromb Haemost*. 2018;16(9):1873-1886.
47. Schillemans M, Karampini E, van den Eshof BL, et al. Weibel-Palade body localized syntaxin-3 modulates Von Willebrand factor secretion from endothelial cells. *Arterioscler Thromb Vasc Biol*. 2018;38(7):1549-1561.
48. van Breevoort D, Snijders AP, Hellen N, et al. STXBP1 promotes Weibel-Palade body exocytosis through its interaction with the Rab27A effector Slp4-a. *Blood*. 2014;123(20):3185-3194.
49. Lenzi C, Stevens J, Osborn D, Hannah MJ, Bierings R, Carter T. Synaptotagmin 5 regulates Ca(2+)-dependent Weibel-Palade body exocytosis in human endothelial cells. *J Cell Sci*. 2019;132(5):jcs221952.
50. Davis GE, Bayless KJ, Mavila A. Molecular basis of endothelial cell morphogenesis in three-dimensional extracellular matrices. *Anat Rec*. 2002;268(3):252-275.
51. Davis GE, Senger DR. Endothelial extracellular matrix: biosynthesis, remodeling, and functions during vascular morphogenesis and neovessel stabilization. *Circ Res*. 2005;97(11):1093-1107.
52. Tetzlaff F, Fischer A. Human endothelial cell spheroid-based sprouting angiogenesis assay in collagen. *Bio-protocol*. 2018;8(17):e2995.
53. Timmins NE, Dietmair S, Nielsen LK. Hanging-drop multicellular spheroids as a model of tumour angiogenesis. *Angiogenesis*. 2004;7(2):97-103.
54. Wang X, Phan DTT, Sobrino A, George SC, Hughes CCW, Lee AP. Engineering anastomosis between living capillary networks and endothelial cell-lined microfluidic channels. *Lab Chip*. 2016;16(2):282-290.
55. Sobrino A, Phan DT, Datta R, et al. 3D microtumors in vitro supported by perfused vascular networks. *Sci Rep*. 2016;6:31589.
56. Norden PR, Kim DJ, Barry DM, Cleaver OB, Davis GE. Cdc42 and k-Ras control endothelial tubulogenesis through apical membrane and cytoskeletal polarization: novel stimulatory roles for GTPase effectors, the small GTPases, Rac2 and Rap1b, and inhibitory influence of Arhgap31 and Rasa1. *PLoS One*. 2016;11(1):e0147758.
57. Norden PR, Sun Z, Davis GE. Control of endothelial tubulogenesis by Rab and Ral GTPases, and apical targeting of caveolin-1-labeled vacuoles. *PLoS One*. 2020;15(6):e0235116.
58. Akerberg AA, Stewart S, Stankunas K. Spatial and temporal control of transgene expression in zebrafish. *PLoS One*. 2014;9(3):e92217.
59. Gore AV, Monzo K, Cha YR, Pan W, Weinstein BM. Vascular development in the zebrafish. *Cold Spring Harb Perspect Med*. 2012;2(5):a006684.
60. Gut P, Reischauer S, Stainier DYR, Arnaout R. Little fish, big data: zebrafish as a model for cardiovascular and metabolic disease. *Physiol Rev*. 2017;97(3):889-938.
61. Lawson ND, Weinstein BM. In vivo imaging of embryonic vascular development using transgenic zebrafish. *Dev Biol*. 2002;248(2):307-318.
62. Simons M. An inside view: VEGF receptor trafficking and signaling. *Physiology (Bethesda)*. 2012;27(4):213-222.

SUPPORTING INFORMATION

Additional supporting information may be found online in the Supporting Information section.

How to cite this article: Francis CR, Kushner EJ. Capturing membrane trafficking events during 3D angiogenic development in vitro. *Microcirculation*. 2022;29:e12726. https://doi.org/10.1111/micc.12726